The Meteoritical Society

Meteoritics & Planetary Science 1–15 (2018)
doi: 10.1111/maps.13231

Reaction of Q to thermal metamorphism in parent bodies: Experimental simulation

A. B. VERCHOVSKY[1*], S. A. HUNT[2], W. MONTGOMERY[3], and M. A. SEPHTON[3]

[1]School of Physical Sciences, The Open University, Walton Hall, Milton Keynes MK7 6AA, UK
[2]Department of Earth Sciences, University College London, Gower Street, London WC1E 6BT, UK
[3]Organic Geochemistry Laboratory, Imperial College London, London SW7 2AZ, UK
[*]Corresponding author. E-mail: sasha.verchovsky@open.ac.uk

(Received 03 October 2017; revision accepted 01 November 2018)

Abstract–Planetary noble gases in chondrites are concentrated in an unidentified carrier phase, called "Q." Phase Q oxidized at relatively low temperature in pure oxygen is a very minor part of insoluble organic matter (IOM), but has not been separated in a pure form. High-pressure (HP) experiments have been used to test the effects of thermal metamorphism on IOM from the Orgueil (CI1) meteorite, at conditions up to 10 GPa and 700 °C. The effect of the treatment on carbon structural order was characterized by Raman spectroscopy of the carbon D and G bands. The Raman results show that the IOM becomes progressively more graphite-like with increasing intensity and duration of the HP treatment. The carbon structural transformations are accompanied by an increase in the release temperatures for IOM carbon and ^{36}Ar during stepped combustion (the former to a greater extent than the latter for the most HP treated sample) when compared with the original untreated Orgueil (CI1) sample. The ^{36}Ar/C ratio also appears to vary in response to HP treatment. Since ^{36}Ar is a part of Q, its release temperature corresponds to that for Q oxidation. Thus, the structural transformations of Q and IOM upon HP treatment are not equal. These results correspond to observations of thermal metamorphism in the meteorite parent bodies, in particular those of type 4 enstatite chondrites, e.g., Indarch (EH4), where graphitized IOM oxidized at significantly higher temperatures than Q (Verchovsky et al. 2002). Our findings imply that Q is less graphitized than most of the macromolecular carbonaceous material present during parent body metamorphism and is thus a carbonaceous phase distinct from other meteoritic IOM.

INTRODUCTION

Primitive meteorites and other pristine extraterrestrial material contain significant amounts of carbon, most of which is present as insoluble organic matter (IOM) (Sephton 2002; Gilmour 2003; Pizzarello et al. 2006). A very minor fraction of the IOM seems to be a carbon-rich phase, called "Q," that has been shown to contain the majority of the planetary noble gases (denoted as Q gases) remaining in the meteoritic material (Lewis et al. 1975; Ott et al. 1981; Schelhaas et al. 1990; Huss et al. 1996; Ott 2014). Almost all of the Q gases can be lost by HNO_3 treatment, but the corresponding weight loss of IOM is small (less than 1%; Lewis et al. 1975) when HNO_3 treatment is performed. Despite the association with IOM there is an additional hypothesis that assigns Q gases to multiple carriers, one of which could be a sulfide such as FeS (Marrocchi et al. 2015). Because FeS exhibits similar responses to HCl and HNO_3 treatment as Q, it should also be oxidized in a pure oxygen atmosphere at low temperature (300–500 °C) as has been observed for Q in HF/HCl residues, an observation that has not been yet made. Moreover, our stepped combustion results for the bulk meteorite and HF/HCl residue samples show that decomposition of FeS or other sulfides occurs at significantly higher (800–1100 °C) temperature than required for oxidation of Q (400–700 °C). This can be traced by the release of SO_2, which is formed in the presence of molecular oxygen (see the 'C, N, and Noble Gas Analyses' section for details).

Despite of all the above findings, the origin and exact chemical nature of Q in chondrites remains an unsolved cosmochemical puzzle. The problem is that Q has not been separated in a pure form and its chemical and physical properties are, therefore, not well characterized. One way to infer the characteristics of Q is to investigate its behavior under different natural processes such as, for example, thermal metamorphism. Thermal metamorphism affects IOM and Q during and following the formation of the meteorite parent bodies (e.g., Huss et al. 2006).

Thermal metamorphism, both on Earth and in meteorite parent bodies, affects the carbon order of carbonaceous material. Primitive IOM is highly disordered and becomes more graphite-like with increasing metamorphic grade. Raman spectroscopy is widely accepted in geo- and cosmo-chemistry as a method to evaluate the grade of metamorphism experienced by organic material in rocks. Higher grades of metamorphism correspond to greater carbon order in the material resulting in narrower D and G Raman peaks at ~1350 cm^{-1} and ~1590 cm^{-1} wavelength, respectively, and appearance of additional band at 1620 cm^{-1} (Pasteris and Wopenka 1991; Wopenka and Pasteris 1993; Beyssac et al. 2002a, 2002b, 2003; Busemann et al. 2007; Busheck and Beyssac 2014). Pure well-crystallized graphite has a single narrow G band, while in contrast, poorly crystallized carbon has wide D and G bands with variable intensity ratios (Pasteris and Wopenka 1991; Wopenka and Pasteris 1993; Beyssac et al. 2002a).

The most effective method by which to study noble gases in meteorites is a stepwise extraction technique, normally using either pyrolysis or combustion, since it allows separation of noble gas components by their release temperature. The latter seems to be more appropriate for carbonaceous carriers such as Q, since noble gas extraction temperature in this case is usually much lower than required by pyrolysis. Combustion can also be used for simultaneous carbon analysis (release pattern and isotopic composition), which is important for identification of the carriers.

The concentration of planetary noble gases in meteorites decreases systematically with increasing metamorphic grade of the meteorite parent body (Huss et al. 1996). This decrease could be due to either the destruction of Q or the nondestructive release of the noble gases from the carrier phase Q. The concentration of the carbonaceous presolar grains such as nanodiamonds and SiC also decreases with increasing metamorphic grade (Huss and Lewis 1995), indicating that oxidation takes place as part of the metamorphism. This transformation, initiated by thermal metamorphism, both destroys IOM and affects Q. In highly metamorphosed meteorites such as Saratov (L4), the ratio of noble gases to carbon remains comparable to (Fisenko et al. 2017) or higher (Matsuda et al. 2010) than that observed in the most primitive meteorites, indicating that Q is destroyed (oxidized) during metamorphism to similar or lesser degree than IOM.

All attempts to separate Q from IOM in pure form have failed (Matsuda et al. 1999; Ott 2014; Marrocchi et al. 2015) because of the very similar chemical properties of the two phases. However, the planetary noble gas carrier, Q, is oxidized by HNO_3 and other oxidizing acids (Lewis et al. 1975; Reynolds et al. 1978; Ott et al. 1981), while most of IOM remains unaffected. This has led to the idea that Q is not a separate phase but rather represents a number of adsorption sites for noble gases within the IOM network (Zadnik et al. 1985). The destruction of Q by HNO_3 or other oxidizing acids while leaving most of IOM unchanged (Lewis et al. 1975; Wieler et al. 1991) could mean that the acid destroys the adsorption sites. Q can also be oxidized in a pure oxygen atmosphere at relatively low temperatures (Ott et al. 1981; Schelhaas et al. 1990; Verchovsky et al. 2002). In this case, its behavior is very similar to the significantly more abundant IOM present in meteorites. In spite of this, there is other evidence that Q and IOM are chemically and physically different phases. The highly metamorphosed Yilmia (EL6) meteorite has IOM that has been converted into much more ordered graphite-like material (see the 'Raman Data' section). The highly ordered material has a higher combustion temperature (>500 °C) than that of IOM from more primitive meteorites (300–500 °C). However, the release of Q noble gases during stepped combustion of Yilmia (EL6) occurs at almost the same temperature (300–500 °C) as for the less metamorphosed meteorites such as Murchison or Orgueil (CI1), indicating that Q has not been graphitized during the strong thermal metamorphism experience by these meteorites (Verchovsky et al. 2002).

In the whole rock CR2 and CR3 meteorites, Q is oxidized during laboratory stepped combustion at a significantly higher temperature than IOM, indicating physical or chemical separation between the two phases (Verchovsky et al. 2012; Verchovsky 2017). However, Q is oxidized simultaneously with IOM in CR meteorites of petrological type 1 and in HF/HCl residues (Grady et al. 2002; Verchovsky et al. 2002; Jenniskens et al. 2012; Verchovsky 2017). Therefore, the low oxidation temperature of Q seems to be its true oxidation temperature when untransformed by secondary processing. In the cases where Q is oxidized at high temperature, there must be a factor preventing direct contact of Q with oxygen during laboratory oxidation. It has been suggested that Q is protected by its

Table 1. Experimental conditions, apparatus, and Raman peak properties for each sample in this study.

Sample	Experimental conditions (where applicable)				Raman peak properties		
	Apparatus	Temperature (°C)	Pressure (GPa)	Duration (hours)	G_D (cm^{-1})	G_G (cm^{-1})	Int D/ Int G
Original Orgueil CI1 HF/HCl	–	–	–	–	293 ± 6	96 ± 1	0.78 ± 0.01
Expt 1	Diamond anvil cell	300	8	8	296 ± 6	92 ± 1	0.76 ± 0.01
Expt 2	Piston-cylinder	500	1	48	85 ± 9	60 ± 2	1.17 ± 0.03
Expt 3	Piston-cylinder	700	1	24	85 ± 2	71 ± 1	1.41 ± 0.03
Expt 4	Piston-cylinder	700	1	72	116 ± 5	52 ± 3	0.81 ± 0.06
Expt 5	Piston-cylinder	700	2	72	95 ± 1	57 ± 2	1.11 ± 0.02
Expt 6	Multi-anvil	700	10	72	46 ± 1	42 ± 3	1.45 ± 0.15
Indarch EH4	–	–	–	–	58 ± 1	36 ± 2	0.80 ± 0.04
Yilmia EL6	–	–	–	–	48 ± 2	20 ± 1	0.16 ± 0.02

The errors on the Raman data are one standard error of the several grain measurements in the same sample.

surroundings in these cases (Verchovsky 2017; Verchovsky et al. 2017). This evidence indicates that Q and IOM are not homogeneously mixed in the matrix of at least some meteorites and occur as distinct materials in different surroundings that determine their oxidization temperature during laboratory stepped combustion. This means that Q and IOM can in principle be physically separated from each other.

In the present study, we reproduced thermal metamorphism of Q and IOM in meteorite parent bodies using high-pressure (HP) and moderate-temperature experiments. Our objective was to explore whether Q and IOM respond differently to thermal metamorphism, thus facilitating their separation during stepped combustion and to compare this response to that of naturally metamorphosed enstatite chondrites.

METHOD

Samples

The samples for the HP experiments were prepared from two whole rock aliquots of Orgueil meteorite (CI1). The samples were treated with HF/HCl to concentrate the carbonaceous IOM and Q phase, similar to that described in Amari et al. (1994). The IOM of Orgueil (CI1) is some of the most primitive carbonaceous material known, being only slightly thermally metamorphosed but substantially altered by water (Zolensky and McSween 1988). Orgueil is the most suitable sample for the high-pressure experiments, since its carbonaceous material is largely represented by disordered carbon (Busemann et al. 2007), which under high pressure and temperature should become more graphite-like. This transformation was monitored using Raman spectroscopy. Once samples were prepared, they were stored at room temperature in air, conditions in which the storage of ^{36}Ar in Q should not be affected. For comparison, we used the data for HF/HCl residues from meteorites Indarch (EH4) and Yilmia (EL6), which have been strongly thermally metamorphosed under reducing conditions on their parent bodies (Keil 1989). A previous study (Verchovsky et al. 2002) indicates that organic matter in these meteorites has been graphitized due to thermal metamorphism and can be oxidized during stepped combustion in the laboratory at a relatively high temperature.

High-Pressure Experiments

Since the time scale of the parent body metamorphism (up to 10s of million years) cannot be reproduced in the laboratory, we sought to achieve the same result in terms of carbon transformation into more structurally ordered forms (as it has been observed in the enstatite chondrites mentioned above), using higher pressures (1–10 GPa) than actually realized in the parent bodies of enstatite chondrites (≤0.1 GPa; Kissin 1989). The maximum temperature used in the experiments was similar or slightly less than that recorded in the enstatite chondrite parent bodies (400–900 °C; Zhang and Sears 1996). A number of high-pressure techniques were used in this study; these methods are described separately below, and the experimental conditions are listed in Table 1.

The samples were sealed in gold capsules to prevent external air from getting to the samples during the experiments. The samples were packed tightly in the capsules which were precompressed to remove as much dead volume (air) as possible from around the sample. The only residual air present in the capsule after its compression is that which remains between the grains. Since the grains are soft and compressible, the amount of air present was minimal. The small amount of O_2

present may be consumed by the sample but it will not be sufficient to react with all the carbonaceous material. The cells were carbon free and composed principally of MgO and Inconel. Under the conditions of the experiments, the Ni-NiO fO_2 buffer is negative but the furnace should not have affected conditions inside the capsules.

Diamond Anvil Cell

A ~10 μg sample of Orgueil (CI1) HF/HCl residue was placed in the gasket hole of a resistively heated (water-jacket cooling) membrane-type diamond anvil cell containing type-II diamonds with 500 μm culets. The stainless-steel gasket had a 200 μm diameter sample chamber and a pre-indented thickness of 30 μm. The sample was compressed to 8 GPa and heated to 300 °C for 8 h. The pressure was determined by ruby fluorescence (Mao et al. 1986) using a chip of ruby placed within the sample chamber. After cooling, the sample was recovered from the gasket by mechanical force and stored in a clean glass vial prior to analysis. The experiment was performed at the Swiss Light Source, Switzerland and further experimental details, including temperature calibration are given by Jennings et al. (2010).

Piston-Cylinder and Multi-Anvil

The piston-cylinder experiments were performed in a half-inch piston-cylinder apparatus (Boyd and England 1960) with an assembly designed to be free of carbon. Sleeves of NaCl with 12.5 mm outer (~1/2 inch) and 5 mm inner diameters combined with a 50 μm thick Inconel furnace. The inner parts of the assembly were all MgO. The sample was placed in the hot-spot of the furnace, immediately adjacent to the thermocouple junction but separated from it by a ~1 mm thick alumina disk. The samples were encapsulated in gold foil and were nominally ~2.5 mm high and ~1.5 mm in diameter, which restricts the sample weight to a few mg. The capsules were compressed before being inserted into the assembly to minimize the amount of air inside the capsule.

A 6–8, octahedral multi-anvil apparatus (similar to that described in Walker et al. 1990) was used for the final experiment. The cell was nominally carbon free, consisting of an 18 mm edge length Cr-doped MgO octahedron, an Inconel furnace inside a ZrO_2 sleeve, and all other cell parts made from MgO. The sample was made in the same way as those for the piston-cylinder. This assembly was compressed by cubic anvils with 11 mm corner truncations.

Both the piston-cylinder and multi-anvil experiments were compressed to the desired end load, heated quickly to the run temperature (~100 °C min^{-1}) before being held at these conditions for the desired length of time, after which the temperature was quenched and the pressure was reduced.

Raman Spectroscopy

The Raman spectroscopy was performed using a Jobin Yvon Labram micro Raman instrument equipped with 532 nm wavelength Nd:YAG laser set to a laser power of ~3 mW. The ×50 objective produces a laser spot size approximately 2 μm in diameter. Only the main D (at about 1350 cm^{-1}) and G (at about 1590 cm^{-1}) carbon bands in the range 1000–2000 cm^{-1} were determined. For each sample, 10 or more spectra were obtained from different carbonaceous grains. In some cases, the spectra were obtained during mapping of small areas (~20 × 20 μm) with spatial resolution 1–2 μm. In order to reduce the thermal effect of the laser beam on the carbonaceous grains only 10% of the total laser power (i.e., ~0.3 mW) was used during sample analyses.

To characterize the degree of structural order in the carbon, the D and G carbon band peaks were fitted with Lorentzian peak functions from which, the full width at half maximum (FWHM) of D abd G bands (designated as Γ_D, Γ_G, respectively) and the ratio of their heights (IntD/IntG) was determined (Table 1). For comparison with the original and HP Orgueil (CI1) samples, Raman spectra were also acquired for HF/HCl residues of the Indarch (EH4) and Yilmia (EL6) meteorites described by Verchovsky et al. (2002).

C, N, and Noble Gas Analyses

The original and HP samples were analyzed by stepped combustion (from 200 to 1400 °C with increments of 100 °C) using the Finesse mass spectrometric complex developed at the Open University (Wright et al. 1988; Verchovsky et al. 1998, 2002; Verchovsky 2017). A detailed description of the analytical protocol can be found in Verchovsky (2017). Amounts and isotopic compositions of the released C (as CO_2), N, Ar, Xe, and He (amounts only) were determined for each temperature step of the combustion. Due to the relatively high concentration of C and N in the sample, the blank corrections for these elements were negligible (~0.1%). The blank corrections for ^{4}He and ^{36}Ar were <10% for the temperature steps within the main peak of their release, and significant (up to 50%) for Xe, depending on the sample size. Amounts of gases in the blank are variable within about 30%, but we run blanks before each series of experiments (see below). Since HF/HCl residue from Orgueil meteorite contains a little, if any, radiogenic

^{40}Ar, it was assumed for blank ^{36}Ar correction that all ^{40}Ar released during analysis is due to contamination of the sample by atmospheric argon during preparation or analysis. The bulk elemental abundances and isotopic composition of each sample were determined by integrating the measured values found at each temperature step.

For each HP experiment, we made mass spectrometry measurements from both the original and HP samples within a short time period (48 h) to minimize systematic errors in the sensitivity and calibration of the Finesse instrument and to avoid systematic offset in the combustion temperature measurements caused by minor variation in the thermocouple position relative to the sample in the extraction furnace. This was particularly important as the HP experiments were performed over a period of 4 yr with significant time intervals (3–12 months) between analyses of separate experiments. Sensitivity calibration can vary slightly over long periods of time.

The amount of CO_2 formed during combustion of carbon-bearing samples is quantified by pressure measurement using calibrated baratron. If sulfides are present in the sample, SO_2 is formed during combustion as well as CO_2. The Finesse instrument cannot separate SO_2 from CO_2 during combustion, consequently the apparent amount of CO_2 measured in this case is higher than actually present. After the baratron measurements, the gas is then split to take a fraction of it into the carbon mass spectrometer for isotope measurement. The amount of CO_2 can also be calculated using the signal on mass 44, mass spectrometer sensitivity, and the gas split factor. The difference in the CO_2 amount found by baratron and mass spectrometric measurements gives the amount of SO_2.

RESULTS

Raman Data

Representative examples of Raman spectra obtained for each sample are presented in Fig. 1. Three spectra are shown for each sample illustrating the variability of the Raman spectra within each sample. Despite this variability, the difference between the spectra for each sample is small compared to the changes in intensity ratios and FWHM of the spectra between samples. The initially broad and overlapping peaks (Fig. 1a) sharpen significantly with increasing temperature, pressure, and duration of the experiments. To quantify the degree of metamorphism, the FWHM and the intensity ratio of D and G Raman bands have been measured (Table 1).

The decreasing width of the D and G peaks with increasing intensity of the HP treatments is shown in Fig. 2. The IOM of Indarch (EH4) and Yilmia (EL6) both have narrower half widths for the G band (Γ_G) than the HP-treated Orgueil (CI1) samples, indicating a higher degree of carbon ordering for the former than the latter. The decrease in Γ_D and Γ_G is broadly correlated (Fig. 3) and Γ_D decreases faster than Γ_G.

The highest variability in the Int D/Int G peak height ratio is observed for the Orgueil (CI1) sample treated at 10 GPa. The ratio ranges between 0.5 and 2.5 and displays a good correlation with Γ_G (Fig. 4). This indicates that within the sample the carbon grains have different structural order. This is not surprising since IOM is a mixture of different organic substances, which have different affinities for graphitization. The higher standard deviations of the Raman parameters shown in the Table 1 for the treated samples compared to the original one can be regarded as a confirmation of the above statement. A similar but steeper correlation is observed for the Indarch (EH4) IOM and an even steeper but less pronounced trend is observed for the Yilmia (EL6) IOM. For this, most strongly thermally metamorphosed sample both Γ_G and Int D/Int G are much smaller compared to the other samples (Fig. 4).

For the sample treated at 700 °C, 10 GPa, and 72 h, an additional peak at about 1620 cm^{-1} as a shoulder on the main peak at 1590 cm^{-1} is observed (Fig. 1g). This shoulder is also seen in the Indarch (EH4) and Yilmia (EL6) spectra (Figs. 1h and 1j). It is not seen in poorly crystallized graphite, since it is not resolved when Raman peaks are broad and is a characteristic of ordered graphitic carbon (Wopenka and Pasteris 1993; Busheck and Beyssac 2014). This is further evidence of higher grade metamorphism in the more treated samples.

Stepped Combustion

Stepped combustion of our metamorphosed samples shows a clear shift of carbon oxidation temperature toward high temperatures compared to the corresponding untreated material (Fig. 5). This is the same for all our samples except the sample treated at 8 GPa and 300 °C, for which we have no data because it was not analyzed by stepped combustion due to the very small sample size. The shift varies from 100 to 200 °C for different HP treatment conditions, with an average ~140 °C. Similar shifts are observed for ^{36}Ar release (Fig. 6). Except for the sample treated at 700 °C and 1 GPa for 72 h (Fig. 6c), the shifts almost follow those observed for carbon (Fig. 5) in terms of their correspondence to the intensity of treatment.

However, since most of the cumulative release curves for the original and treated samples are not parallel, the temperature shift is variable and depends on the yield of C and ^{36}Ar (Figs. 5 and 6). This makes

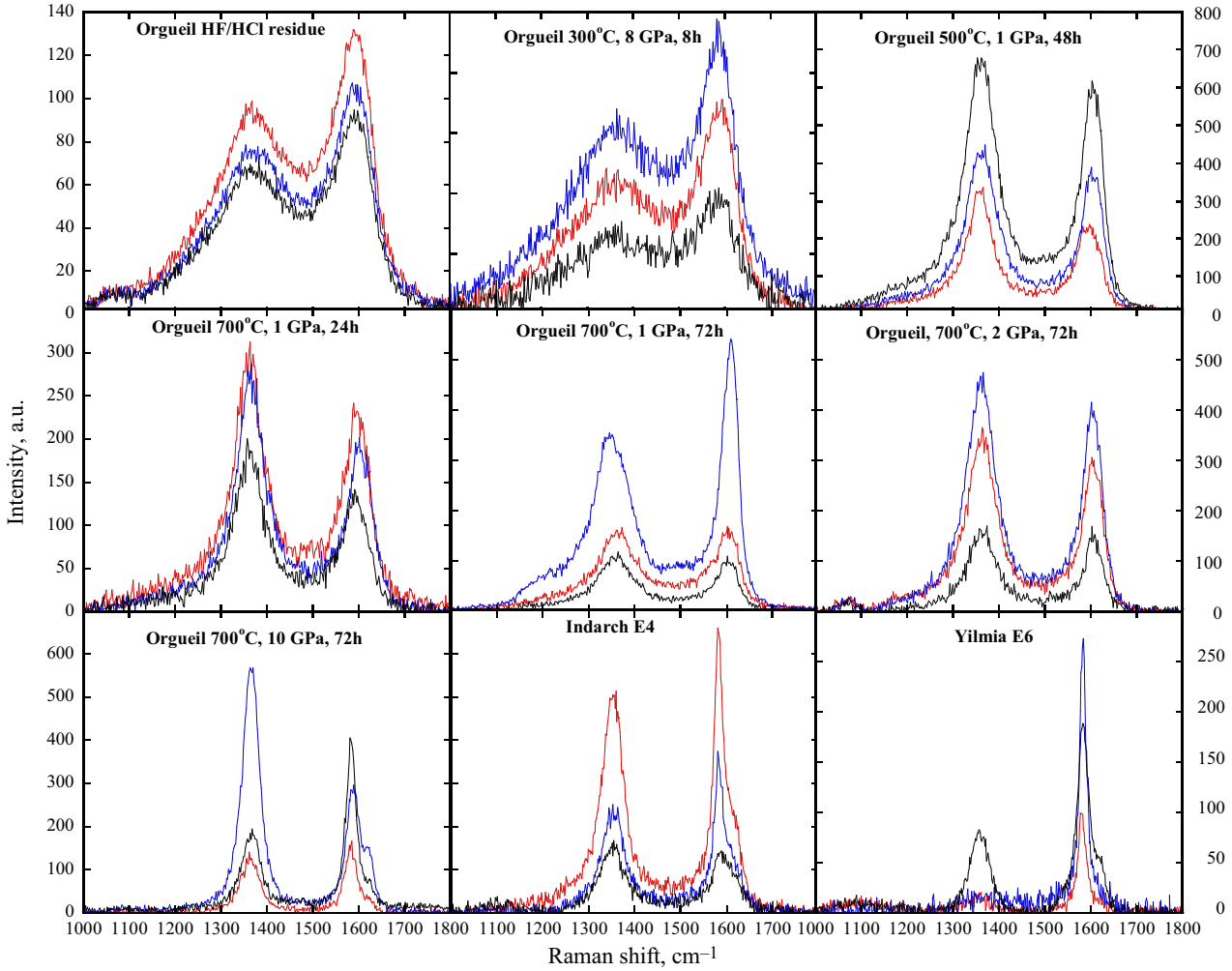

Fig. 1. Examples of Raman spectra for the original and recovered samples from Orgueil meteorite (CI1) as well as those from the Indarch (EH4) and Yilmia (EL6) meteorites. D and G bands are observed at 1340–1360 and 1580–1600 cm^{-1}, respectively for all the samples. The three spectra for each sample illustrate the variability in the ratio of the D/G intensity bands.

it difficult to quantitatively evaluate an average shift for each sample. Therefore, we suggest using the total area between the curves for the original and HP samples as a quantitative measure of the temperature shift (ΔT_C and ΔT_{Ar} for C and ^{36}Ar, respectively) (Figs. 5 and 6). Indeed, the larger the area between the curves, the bigger the average temperature shift. We assume that the total areas between the two curves and the average temperature shifts are connected by a linear function. In order to translate the areas into temperature shifts the linear function needs to be calibrated. The C stepped combustion data for the sample treated at 10 GPa, 700 °C for 72 h (Fig. 5e) can be used for calibration, since the curves for the original and treated samples are almost parallel to each other. We assumed that the average temperature shift for this sample is 127 ± 10 °C as observed at 40% yield. The area into temperature shift-translation coefficient determined for the sample was applied to all other samples. The results are presented in Table 2. We conservatively estimate the errors for the temperature shifts to ~15%. The main source of uncertainty is the temperature shift for carbon for the sample that was used for calibration.

Variations of ΔT_C and ΔT_{Ar} with intensity of treatment do not show a regular trend, though the least treated sample (500 °C, 1 GPa, 48 h) has the smallest ΔT_C (Fig. 7). Following HP treatment at 700 °C, 1 GPa for 72 h, the negative shift in ΔT_{Ar} means that, in contrast to all other samples, ^{36}Ar release in this sample occurs at a temperature that is lower than in the untreated sample and in this sense can be considered as an anomalous.

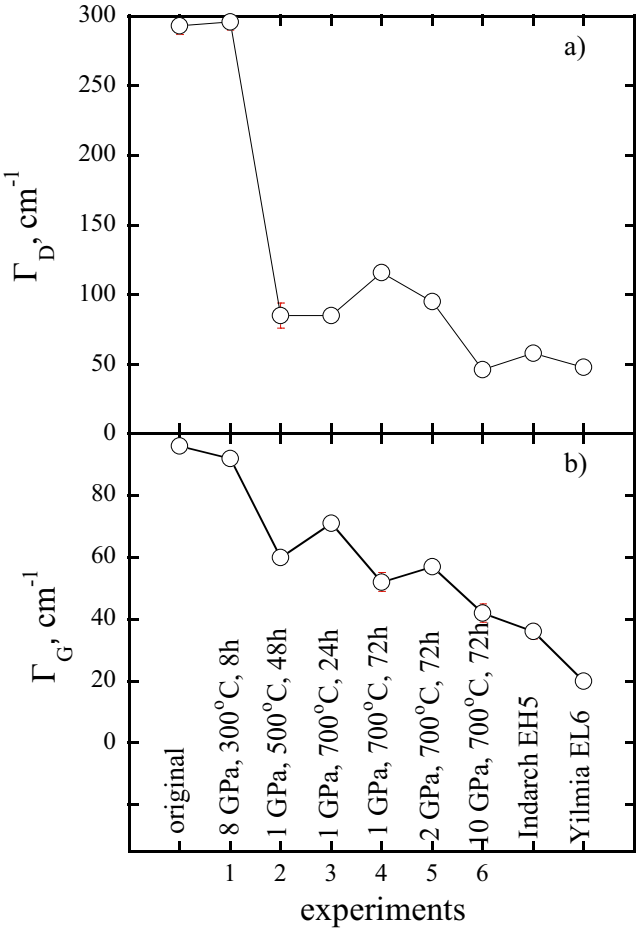

Fig. 2. Variations of the Raman parameters ΓD and ΓG for the original and treated at HP Orgueil (CI1) HF/HCl residues. The samples are arranged in an array (from 1 to 6) with increasing intensity of the treatment. The results for HF/HCl residues from Indarch (EH4) and Yilmia (EL6) are also included.

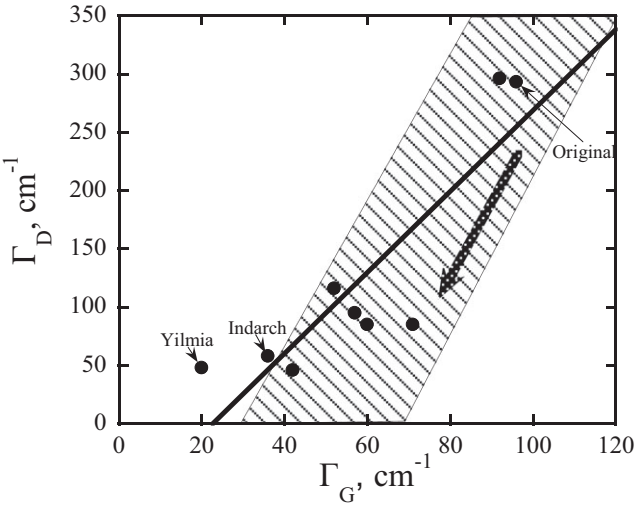

Fig. 3. Correlation between ΓG and ΓD Raman parameters for the IOM from Orgueil (CI1) (original and HP), Indarch (EH4), and Yilmia (EL6). The shadow area corresponds to the trend found for IOM from a large number of primitive meteorites (Busemann et al. 2007). The arrow within the shadow area indicates the direction of increasing degree of thermal metamorphism in the parent bodies of the meteorites. The solid line is the linear fit for the experimental points. Errors are smaller than the symbols.

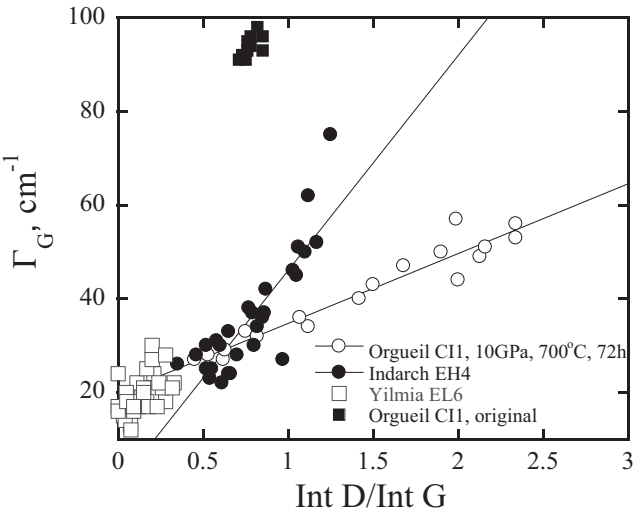

Fig 4. Correlations between GG and the intensity ratio of D and G bands for the Orgueil (CI1) IOM treated at 10 GPa and IOM from Indarch (EH4), Yilmia (EL6), and Orgueil (CI1) original samples. With increasing degree of thermal metamorphism, the correlations become steeper, since the average Int D/Int G ratio decreases.

The variations of the ^{36}Ar/C ratio in combustion steps (Fig. 8) for the original and treated samples remain almost parallel within the range of the main carbon release. Deviations from this behavior are observed only at the beginning of combustion at less than 10% of carbon release where ^{36}Ar/C ratios are systematically higher (except for the sample treated at 700 °C and 1 GPa for 24 h (Fig. 8b).

Bulk Concentrations of Noble Gases, Carbon, and Nitrogen

Bulk chemical abundances of C, N, and the noble gases in our samples were calculated from the stepped combustion data and are presented in Table 3. Two of the samples have significantly reduced carbon content compared with the original material. This is likely to be caused by an analytical artifact where meteorite carbon is diluted with non meteoritic material (gold capsule). For this reason and since the dilution effect

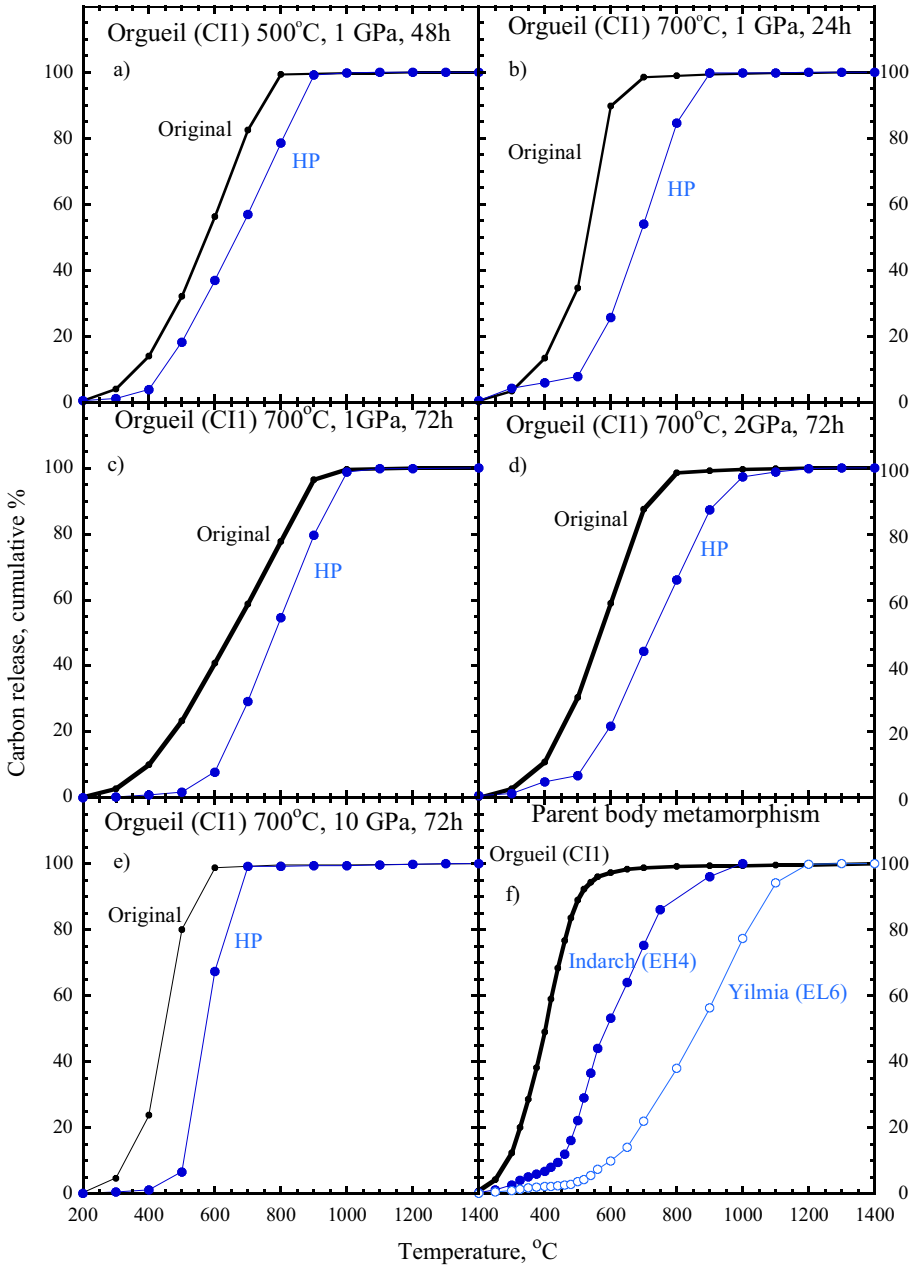

Fig. 5. Carbon cumulative release for the HP treated and original IOM from Orgueil (CI1) samples analyzed at the same time. The data for HF/HCl residues from Orgueil (CI1), Indarch (EH4), and Yilmia (EL6) from Verchovsky et al. (2002) are also included for comparison.

affects C and noble gas concentrations equally, we normalize concentrations to the carbon content of the sample.

Several factors must be taken into account in the interpretation of the abundance and isotope data. First, nitrogen and noble gases could have been lost as a result of the HP treatments, resulting in decreased concentrations. Atmospheric oxygen can cause oxidation of the IOM, which will also result in a decrease of C and other gas concentrations in line with the natural processes in the parent bodies. The residual atmospheric gases (N_2, ^{40}Ar, and Xe) in the sample capsule could be trapped during HP treatment, leading to an increase in concentration of these gases, while the residual atmospheric oxygen can cause oxidation of the IOM and Q, resulting in the decrease of C and nitrogen and noble gas concentrations. We, however, consider the oxidation effect to be almost negligible, though

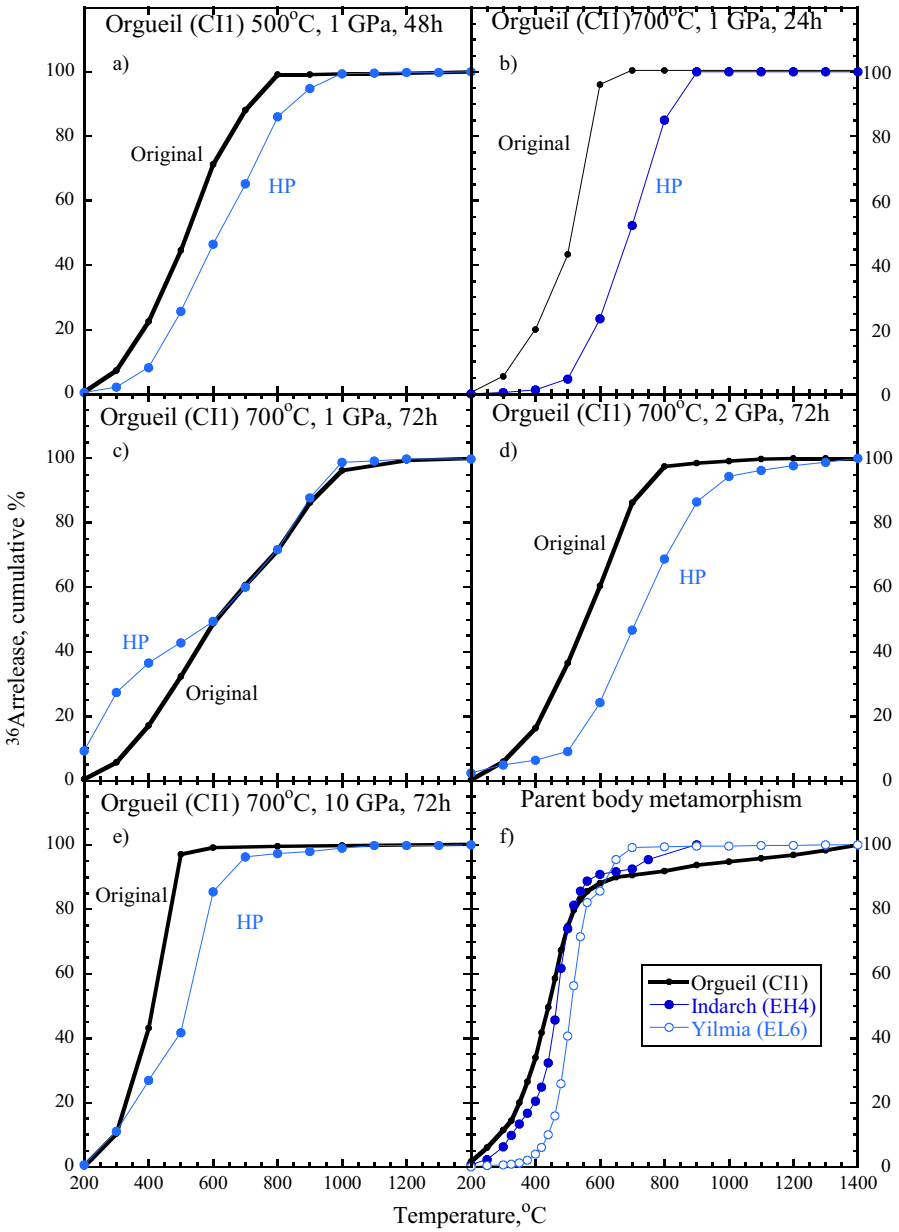

Fig. 6. ^{36}Ar cumulative release for the HP treated and original IOM from Orgueil (CI1) samples analyzed at the same time. The data for HF/HCl residues from Orgueil (CI1), Indarch (EH4), and Yilmia (EL6) from Verchovsky et al. (2002) are also included for comparison.

trapping of atmospheric gases can affect N, C, and Ar isotopic compositions. Finally, because small aliquots of the sample were used in these measurements, variation in results may reflect inhomogeneity of the sample. This is seen for the samples prepared in two different batches (Table 3, the sample used for treatment at 300 °C and all others). Nevertheless, the noble gases, and carbon and nitrogen concentrations in the HP Orgueil (CI1) samples display systematic changes with treatment conditions although there are some exceptions.

The HP samples have systematically lower concentrations of ^{36}Ar than the original samples, while C, N, ^{4}He, and ^{132}Xe show both higher and lower concentrations in the HP samples compared to the original ones (Table 3). Therefore, below we do not consider the gases such as ^{40}Ar, N, and Xe that can be trapped from the residual atmosphere. Four samples, three of them treated at 700 °C for 72 h and one at 500 °C for 48 h, have trapped additional atmospheric Xe, as seen in the C-normalized

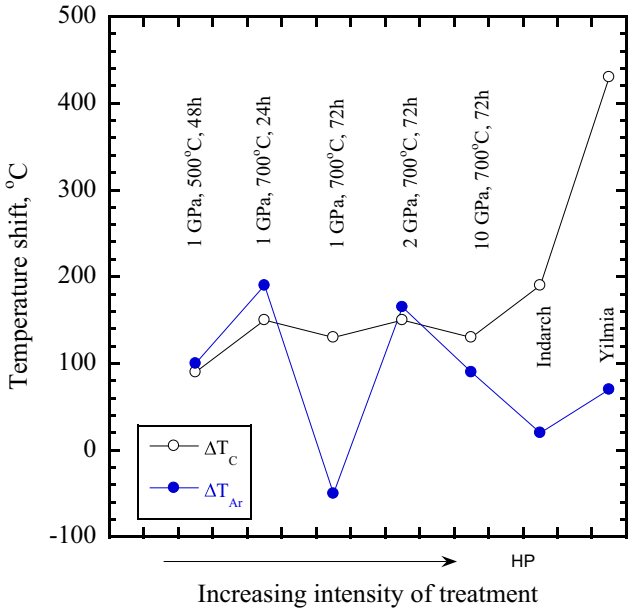

Fig. 7. The temperature shift of C and ^{36}Ar release for the Orgueil (CI1) samples determined as the area between the release curves for the original and treated samples (Figs. 5 and 6) analyzed at the same time. The negative ΔTAr for the sample treated at 700°C and 1 GPa for 72 h indicates that ^{36}Ar release from the sample occurred at lower temperature than that for the original sample that seems to be anomalous with respect to other samples. The corresponding data for Indarch (EH4) and Yilmia (EL6) from Verchovsky et al. (2002) are also included for comparison.

concentrations. The ^{36}Ar concentrations are corrected for atmospheric Ar, and variations in ^{36}Ar should therefore only reflect losses during the treatment, which is actually observed. Indeed, ^{36}Ar/C is smaller in all treated samples compared to the original untreated samples. The ^{36}Ar/C variations normalized to those of the original samples (or the fraction of ^{36}Ar preserved) are within 0.3–0.9, however, do not show any trend with intensity of treatment (Table 2; Fig. 9), in contrast to the clear trend observed for the corresponding Raman parameters. One of the reasons for that could be pressure-induced destruction of carbonaceous material occurring concurrently with loss of ^{36}Ar, which is seen in the increase of ^{36}Ar preservation for the samples treated at the same temperature (700 °C) and duration (72 h) but different pressure.

DISCUSSION

We have performed experiments to simulate thermal metamorphism in the parent bodies of meteorites using IOM from the Orgueil (CI1) meteorite. With increasing pressure, time, and duration, Raman data (Figs. 1–3) indicate that carbon becomes progressively more ordered, i.e., more graphite-like. It is important to emphasize here that the obtained Raman spectra are related exclusively to the bulk IOM, but not to Q, since the relative abundance of the latter, compared to that for rest of the IOM, is extremely low (Lewis et al. 1975; Wieler et al. 1991). However, structural transformations seem to occur in the Q phase as well that can be seen indirectly in the temperature shifts of ^{36}Ar release (Fig. 6), which accompanies the corresponding shifts of the IOM carbon release (Fig. 5). Theoretically, carbon with a more graphite-like structure will be oxidized more slowly and at a higher temperature than carbon with an amorphous structure. Therefore, without structural transformations of the carbonaceous phases (IOM and Q), no differences in the release temperature of carbon and ^{36}Ar would be detected between the HP samples and the original Orgueil (CI1) sample.

The Raman data reveal that the original Orgueil (CI1) sample has a metamorphic grade equivalent to that of kerogen or coal (Wopenka and Pasteris 1993), while the Orgueil (CI1) sample treated at 700 °C and 10 GPa for 72 h corresponds to rocks which have experienced chlorite grade metamorphism (Pasteris and Wopenka 1991; Wopenka and Pasteris 1993; Beyssac et al. 2002a, 2002b). The other samples exhibit lower degrees of metamorphism equivalent to rocks with metamorphic grades between kerogen/coal and chlorite facies.

It is more interesting, however, to compare the results of the experimental simulation with enstatite chondrites Indarch (EH4), and EL6, Yilmia, which underwent thermal metamorphism under reducing conditions (Keil 1989). As mentioned above, in our experiments we used comparable temperatures, higher pressures, and significantly shorter time scale than were experienced during metamorphism in the parent bodies of enstatite chondrites (Kissin 1989; Zhang and Sears 1996). Nevertheless, the overall experimental conditions seem to be strong enough to reproduce parent body metamorphism corresponding to enstatite chondrites of petrological type 4, like Indarch (EH4). Indeed, the Raman parameters for Orgueil (CI1) treated to the highest pressure and temperature (700 °C, 10 GPa, 72 h) approach those established for the Indarch (EH4) IOM (Figs. 2–4); both samples also show the D2 band at 1620 cm^{-1}. Similarities between Orgueil (CI1) treated at 700 °C, 10 GPa, and 72 h and Indarch (EH4) are also evident for the fraction of ^{36}Ar preserved (Fig. 9) and the relative release temperature of carbon and ^{36}Ar (ΔT_C and ΔT_{Ar}) (Fig. 7) that are comparable for the laboratory and naturally metamorphosed samples. On the other hand, the overall experimental conditions did

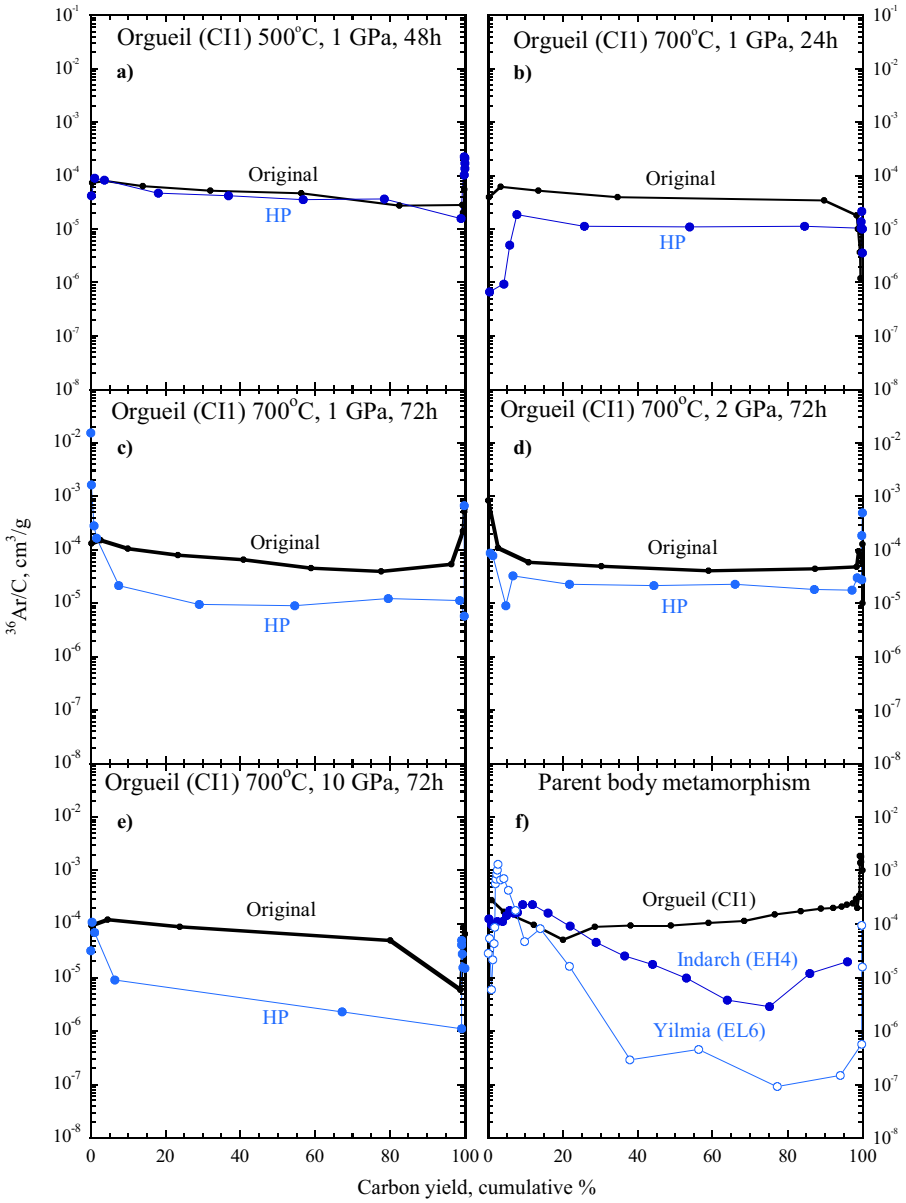

Fig. 8. Variation of ^{36}Ar/C ratio during combustion of the Orgueil (CI1) IOM in the original and HP-treated samples analyzed at the same time. The data for Indarch (EH4) and Yilmia (EL6) from Verchovsky et al. (2002) are also included for comparison.

not reproduce metamorphism in the parent bodies of enstatite chondrites of petrological type 6, based on a comparison with Yilmia (EL6) IOM. Of the samples in this study, Yilmia (EL6) has the lowest ^{36}Ar preservation (Fig. 7), the lowest Raman average Γ_G and Int D/Int G parameters (Figs. 2 and 4), and the highest carbon release temperature (Fig. 7). This seems to be due to a higher degree of equilibration between different organic compounds achieved at such a high-grade parent body metamorphism.

Carbon (from IOM) and ^{36}Ar (from Q) are partly separated from each other in the HP samples. This can be seen in the stepped combustion results which show elevated ^{36}Ar/C ratios in the steps corresponding to the first ≤10% of carbon release (Figs. 8c, 8d, and 8e). A similar but more pronounced effect is also observed for Indarch (EH4) and Yilmia (EL6) (Fig. 8f). The separation of Q and IOM is also confirmed by analysis of the carbon and ^{36}Ar release temperature shifts to higher values for the HP treated Orgueil (CI1) samples.

Table 2. ^{36}Ar retention and C and Ar release temperature shifts.

Sample	Fraction of ^{36}Ar preserved[a]	ΔT_C (°C)	ΔT_{Ar} (°C)
300 °C, 8 GPa, 8 h	0.30	–	–
500 °C, 1 GPa, 48 h	0.89	90 ± 14	100 ± 15
700 °C, 1 GPa, 24 h	0.30	150 ± 23	190 ± 29
700 °C, 1 GPa, 72 h	0.28	130 ± 20	−50 ± 8[b]
700 °C, 2 GPa, 72 h	0.46	150 ± 23	165 ± 25
700 °C, 10 GPa, 72 h	0.62	130 ± 20	90 ± 14
Indarch EH4	0.31	190 ± 29	20 ± 3
Yilmia EL6	0.24	430 ± 65	70 ± 11

[a]Calculated as the ratio of ^{36}Ar/C in the sample to the corresponding ratio in the original sample analyzed at the same time. The results for Indarch (EH4) and Yilmia (EL6) are obtained from the data published in Verchovsky et al. (2002).

[b]Negative temperature shift for the sample treated at 700 °C, 1 GPa for 72 h means that ^{36}Ar from the treated sample is released ahead of that from the original one in contrast to all other samples.

Indeed, the shifts, expressed as ΔT_C and ΔT_{Ar}, are not equal, with ΔT_C being both higher and lower than ΔT_{Ar} (Fig. 7; Table 2). As a measure of the separation between carbon and ^{36}Ar, the difference between the corresponding shifts (ΔT_C-ΔT_{Ar}) can be used. Excluding the anomalous sample treated at 700 °C, 1 GPa, and 72 h (Fig. 7), this difference is correlated with the parameter Γ_G (Fig. 10). It is important to emphasize that the HP-treated samples, for which thermal metamorphism has been simulated in the laboratory, and the natural samples, thermally metamorphosed in their parent bodies, form a single trend (Fig. 10). Such single trends for the artificially metamorphosed and metamorphosed in nature samples are also observed for Γ_G and Γ_D (Figs. 2b and 3).

Thus, we conclude that experimental simulation of the parent body metamorphism does result in carbonaceous matter transformation (graphitization) similar to that which has occurred naturally in the meteorite parent bodies (Verchovsky et al. 2002). The only observed difference between the natural and laboratory HP samples is in the degree of transformation.

The simplest explanation for the elevated ^{36}Ar/C at the beginning of combustion (Figs. 8c, 8d, and 8e) and the trend in Fig. 10 is that the carrier of ^{36}Ar, namely the Q phase, is more resistant to graphitization than most of the IOM. Indeed, the parameter Γ_G determines the degree of carbon order/graphitization, while ΔT_C-ΔT_{Ar} defines the difference in the release temperature of the IOM carbon and ^{36}Ar from Q, i.e., in essence the difference in the oxidation temperature of IOM and Q. When ΔT_C-ΔT_{Ar} is negative, Ar releases ahead of carbon and vice versa. The sample treated at 700 °C, 10 GPa for 72 h has a positive ΔT_C-ΔT_{Ar}. Even higher positive values are observed for Indarch (EH4) and Yilmia (EL6). The correlation (Fig. 10) indicates that the higher the degree of graphitization/metamorphism of IOM, the higher the difference between release temperature of carbon and ^{36}Ar, or between the oxidation temperature of IOM and Q. In other words, the oxidation temperature of Q does not increase as much as that of IOM with increasing of metamorphic grade. This would not be observed if IOM and Q have the same ability for graphitization. Thus, we conclude that Q is less susceptible to graphitization than the bulk of IOM. This has been suggested before based on analyses of naturally metamorphosed meteorite samples (Verchovsky et al. 2002) and now is confirmed by the results of our HP experimental simulation.

CONCLUSIONS

Experimental simulation of thermal metamorphism in parent bodies applied to the IOM separated from Orgueil (CI1) results in progressive transformation of carbon into more structurally ordered forms. The IOM becomes more graphite-like, which has been confirmed by Raman spectroscopy. This transformation to a more graphitic character also leads to an increase in the oxidation temperature of the majority of the IOM carbon and a corresponding but smaller increase in the ^{36}Ar release temperature during oxidation of its carrier, the Q phase, for the most metamorphosed sample. It means that IOM and Q react differently to HP treatment and following simulated metamorphism, the resulting materials are not the same in terms of degree of graphitization: Q carbon is more resistant to graphitization than IOM. Thus, the experimental simulation results confirm the conclusion made by analyses of enstatite chondrites of petrological types 4 and 6 (Verchovsky et al. 2002), suggesting that Q and IOM are two chemically different carbonaceous substances with differing abilities to be graphitized during the metamorphization of their parent bodies.

Acknowledgments—The authors are grateful to the Swiss Light Source, Switzerland for synchrotron access, and especially to Philippe Lerch, the beamline scientist at X01DC. We are also grateful to A. V. Fisenko and L. F. Semenova from Vernadsky Institute, Moscow, for the preparation of the HF/HCl residue from Orgueil (CI1). S. A. H. was funded by NERC grants NE/

Table 3. Bulk concentrations of C, N, and noble gases in the HP and original Orgueil (CI1) HF/HCl residues with some isotope data.

Sample	Weight (mg)	C (%)	$d^{13}C$ (‰)	N (ppm)	$\delta^{15}N$ (‰)	^{4}He ($cm^3\ g^{-1}$)	$^{4}He/C$ ($mL\ g^{-1}$)	^{36}Ar ($cm^3\ g^{-1}$)	$^{36}Ar/C$ ($cm^3\ g^{-1}$)	$^{40}Ar/C$ ($cm^3\ g^{-1}$)	$\frac{^{40}Ar}{^{36}Ar}$	^{132}Xe ($cm^3\ g^{-1}$)	$^{132}Xe/C$ ($cm^3\ g^{-1}$)	$\frac{^{129}Xe}{^{132}Xe}$
Original	0.032	64.2	−24.2	14300	6.2	n.a	n.a.	3.28e-05	5.11e-05	0.00031	6.1	1.50e-07	2.34e-07	n.a.
300 °C, 8 GPa, 8 h	0.007	64.8	−29.6	47700	3.4	n.a.	n.a.	1.00e-05	1.54e-05	0.00120	78	8.71e-08	1.34e-07	n.a.
Original	0.749	51.1	−14.3	23500	29.6	3.311e-04	6.485e-04	2.16e-05	4.24e-05	0.00016	3.8	8.29e-10	1.62e-09	n.a.
500 °C, 1 GPa, 48 h	0.697	54.2	−14.8	29800	18.9	4.060e-04	7.489e-04	2.04e-05	3.76e-05	0.00019	5.1	1.31e-09	2.42e-09	n.a.
Original	0.139	48.9	−18.5	13400	18.8	1.230e-03	2.518e-03	1.74e-05	3.56e-05	0.00019	5.2	1.36e-07	2.78e-07	1.041
700 °C 1 GPa, 24 h	0.390	75.8	−15.6	7440	16.3	1.390e-03	1.833e-03	8.00e-06	1.06e-05	0.00006	5.7	6.13e-08	8.08e-08	1.045
Original	0.694	44.2	−14.7	13000	22.3	1.671e-03	3.782e-03	3.04e-05	6.88e-05	0.00032	4.7	6.83e-09	1.55e-08	1.052
700 °C, 1 GPa, 72 h	3.448	5.5	−15.7	733	14.9	6.555e-05	1.183e-03	1.07e-06	1.93e-05	0.00200	104	1.19e-08	2.15e-07	1.031
Original	0.374	45.5	−17.0	12900	23.4	1.198e-03	2.635e-03	2.18e-05	4.79e-05	0.00015	3.1	1.31e-08	2.88e-08	1.061
700 °C, 2 GPa, 72 h	0.646	11.8	−17.0	6330	24.7	2.167e-04	1.841e-03	2.57e-06	2.18e-05	0.00064	29	7.76e-09	6.59e-08	1.018
Original	0.748	41.8	−14.8	n.a.	n.a	5.174e-04	1.239e-03	2.47e-05	5.16e-05	0.00033	6.4	7.71e-09	1.85e-08	1.043
700 °C, 10 GPa, 72 h	0.348	55.8	−15.4	4140	15.4	2.902e-04	5.203e-04	1.78e-06	3.18e-06	0.00067	211	1.59e-08	2.85e-08	1.034

The uncertainties for noble gas and nitrogen concentrations are about 10%, for carbon—$\sim$1%. Isotopic compositions of C and N have errors ~0.5‰.
Only Xe isotope ratio for the most abundant isotopes ($^{129}Xe/^{132}Xe$) is shown because of low precision of measurements for the other isotope ratios.

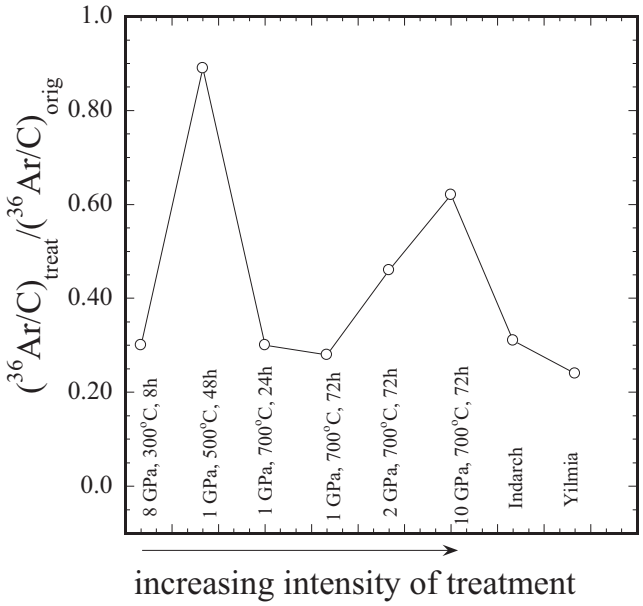

Fig. 9. Preservation of ^{36}Ar in the treated samples depending on the intensity of treatment. The data for Indarch (EH4) and Yilmia (EL6) taken from Verchovsky et al. (2002) normalized for that for Orgueil (CI1) are also included.

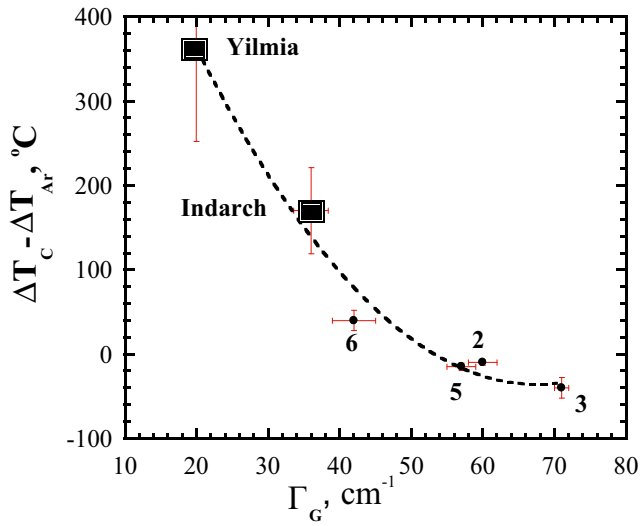

Fig. 10. Correlation of differences in the temperature shifts between C (ΔTC) and ^{36}Ar (ΔTAr) (see Table 2) with the Raman parameter ΓG. The data for Indarch (EH4) and Yilmia (EL6) are also shown. The anomalous sample treated at 700°C, 1 GPa for 72 h is not included. The figures next to the points correspond to the experiment number from the Table 1.

H016309/1 and NE/L006898/1. W. M. and M. A. S. acknowledge support from STFC, grant number ST/K000551/1. We thank two anonymous reviewers for their comments which significantly improved the manuscript.

Editorial Handling—Dr. A. J. Timothy Jull

REFERENCES

Amari S., Lewis R. S., and Anders E. 1994. Interstellar grains in meteorite: I. Isolation of SiC, graphite and diamond: Size distribution of SiC and graphite. *Geochimica at Cosmochimica Acta* 58:459–470.

Beyssac O., Goffe B., Chopin C., and Rouzaud J. N. 2002a. Raman spectra of carbonaceous material in metasidements: A new geothermometer. *Journal of Metamorphic Geology* 20:859–871.

Beyssac O., Rouzaud J. N., Goffe B., Brunet F., and Chopin C. 2002b. Graphitisation in a high-pressure, low-temperature metamorphic gradient: A Raman microspectroscopy and HRTEM stady. *Contributions to Mineralogy and Petrology* 143:19–31.

Beyssac O., Brunet F., Petitet J.-P., Goffe B., and Rouzaud J. N. 2003. Experimental study of the microtextural and structural transformation of carbonaceous materials under pressure and temperature. *European Journal of Mineralogy* 15:937–951.

Boyd F. R. and England J. L. 1960. Apparatus for phase-equilibrium measurements at pressures up to 50 kilobars and temperatures up to 1750 & °C. *Journal of Geophysical Research* 65:741–748.

Busemann H., Alexander C. M. O'D., and Nittler L. R. 2007. Characterization of organic matter in primitive meteorites my microRaman spectroscopy. *Meteoritics & Planetary Science* 42:1387–1416.

Busheck P. R. and Beyssac O. 2014. From organic matter to graphite: Graphitization. *Elements* 10:421–426.

Fisenko A. V., Verchovsky A. B., and Semjonova L. F. 2017. Correlation analysis of the C, N and noble gases released during oxidation of acid resistant fractions separated from the Saratov (L4) meteorite (abstract #1280). 48th Lunar and Planetary Science Conference. CD-ROM.

Gilmour I. 2003. Structural and isotopic analysis of organic matter in carbonaceous chondrites. In *Meteorites, comets, and planets*, edited by Davies A. M. Treatise on Geochemistry, vol. 1. Amsterdam: Elsevier. pp. 269–280.

Grady M. M., Verchovsky A. B., Franchi I. A., Wright I. P., and Pilinger C. T. 2002. Light element geochemistry of the Tagish Lake CI2 chondrite: Comparison with CI1 and CM2 meteorites. *Meteoritics & Planetary Science* 37:719–735.

Huss G. R. and Lewis R. S. 1995. Presolar diamond, SiC, and graphite in primitive chondrites: Abundances as a function of meteorite class and petrologic type. *Geochimica et Cosmochimica Acta* 59:115–160.

Huss G. R., Lewis R. S., and Hemkin S. 1996. The "normal planetary" noble gas component in primitive chondrites: Compositions, carrier, and metamorphic history. *Geochimica et Cosmochimica Acta* 59:3311–3340.

Huss G. R., Rubin A. E., and Grossman J. N. 2006. Thermal metamorphism in chondrites. In *Meteorites and the early solar system II*, edited by Lauretta D. S., Leshin L. A., and McSween H. Y. Jr. Tucson, Arizona: The University of Arizona Press. pp. 567–586.

Jennings E., Montgomery W., and Lerch P. 2010. Stability of coronene at high temperature and pressure. *Journal of Physical Chemistry B* 114:15,753–15,758.

Jenniskens P., Fries M. D., Yin Q., Zolensky M. E., Krot N., Sandford S. A., Sears D., Beauford R., Ebel D. S., Friedrich J. M., Nagashima K., Wimpenny J., Yamakawa A., Nishiizumi K., Hamajima Y., Caffee M. W., Welton K. C., Laubenstein M., Davis A. M., Simon S. B., Heck P. R., Yuong E. D., Kohl I. E., Thiemens M. H., Hunn M. H., Mikouchi T., Hagiya K., Ohsumi K., Cahill T. A., Lowton J. A., Barnes D., Steele A., Rochette P., Verosub K. L., Gattacceca J., Cooper G., Glavin D. P., Burton A. S., Dworkin J. P., Elsila J. E., Pizzarello S., Ogliore R., Schmitt-Kopplin P., Harir M., Hertkorn N., Verchovsky A., Grady M., Nagao K., Okazaki R., Takechi H., Hiroi T., Smith K., Siber E. A., Brown P. G., Albers J., Klotz D., Hankey M., Matson R., Fries J. A., Walker R. J., Puchtel I., Lee C. A., Erdman M. E., Eppich G. R., Roeske S., Gabelica Z., Lerche M., Nuevo M., Girten B., and Worden S. P. (the Sutters's Mill Meteorite Consortium). 2012. Radar-enabled recovery of the Sutter's Mill meteorite, a carbonaceous chondrites regolith breccia. *Science* 338:1583–1587.

Keil K. 1989. Enstatite meteorites and their parent bodies. *Meteoritics* 24:195–208.

Kissin S. A. 1989. Application of the sphalerite cosmobarometer to the enstatite chondrites. *Geochimica et Cosmochimica Acta* 53:1649–1655.

Lewis R. S., Srinivasan B., and Anders E. 1975. Host phase of a strange xenon component in Allende. *Science* 190:1251–1262.

Mao H. K., Xu J., and Bell P. M. 1986. Calibration of the ruby pressure gauge to 800 kbar under quasi-hydrostatic conditions. *Journal of Geophysical Research, Solid Earth* 91:4673–4676.

Marrocchi Y., Avice G., and Estrade N. 2015. Multiple carriers of Q noble gases in primitive meteorites. *Geophysical Research Letters* 42:2093–2099.

Matsuda J., Amari S., and Nagao K. 1999. Purely physical separation of a small fraction of the Allende meteorite that is highly enriched in noble gases. *Meteoritics & Planetary Science* 34:129–136.

Matsuda J., Tsukamoto H., Miyakawa C., and Amari S. 2010. Noble gas study of the Saratov L4 chondrite. *Meteoritics & Planetary Science* 45:361–372.

Ott U. 2014. Planetary and pre-solar noble gases in meteorites. *Chemie der Erde* 74:519–544.

Ott U., Mack R., and Chang S. 1981. Noble-gas-rich separates from the Allende Meteorite. *Geochimica et Cosmochimica Acta* 45:1751–1788.

Pasteris J. D. and Wopenka B. 1991. Raman spectra of graphite as indicators of degree of metamorphism. *Canadian Mineralogist* 29:1–9.

Pizzarello S., Cooper G. W., and Flynn G. J. 2006. The nature and distribution of the organic material in carbonaceous chondrites and interplanetary dust particles. In *Meteorites and the early solar system II*, edited by Lauretta D. S., Leshin L. A., and McSween H. Y. Jr. Tucson, Arizona: The University of Arizona Press. pp. 625–651.

Reynolds J. H., Frick U., Neil J. M., and Phinney D. 1978. Rare-gas-rich separates from carbonaceous chondrites. *Geochimica et Cosmochimica Acta* 42:1775–1798.

Schelhaas N., Ott U., and Begemann F. 1990. Trapped noble gases in unequilibrated ordinary chondrites. *Geochimica et Cosmochimica Acta* 54:2869–2882.

Sephton M. A. 2002. Organic compounds in carbonaceous chondrites. *Natural Products Report* 19:292–311.

Verchovsky A. B. 2017. Origin of isotopically light nitrogen in meteorites. *Geochemistry International* 55:969–983.

Verchovsky A. B., Fisenko A. V., Semjonova L. F., Wright I. P., Lee M. R., and Pillinger C. T. 1998. C, N, and noble gas isotopes in grain size separates of presolar diamonds from Efremovka. *Science* 281:1165–1168.

Verchovsky A. B., Sephton M. A., Wright I. P., and Pillinger C. T. 2002. Separation of planetary noble gas carrier from bulk carbon in enstatite chondrites during stepped combustion. *Earth and Planetary Science Lettters* 199:243–255.

Verchovsky A. B., Pearson V. K., Fisenko A. V., Semjenova L. F., Sephton M. A., and Wright I. P. 2012. Separation of Q from carbon in CR meteorites during stepped combustion (abstract #2645). 43th Lunar and Planetary Science Conference. CD-ROM.

Verchovsky A. B., Fisenko A. V., and Semjonova L. F. 2017. Isotopically light nitrogen in the Q-enriched fractions separated from the Saratov L4 chondrite (abstract #2226). 48th Lunar and Planetary Science Conference. CD-ROM.

Walker D., Carpenter M. A., and Hitch C. M. 1990. Some simplifications to multianvil devices for high pressure experiments. *American Mineralogist* 75:1020–1028.

Wieler R., Anders E., Baur H., Lewis R. S., and Signer P. 1991. Noble gases in "phase Q"; closed-system etching of an Allende residue. *Geochimica et Cosmochimica Acta* 55:1709–1722.

Wopenka B. and Pasteris J. D. 1993. Staructural ccharacterization of kerogens to granulite-facies graphite: Applicability of Raman microprobe soectroscopy. *American Mineralogist* 78:533–557.

Wright I. P., Boyd S. R., Franchi F. A., and Pillinger C. T. 1988. High-precision determination of nitrogen stable isotope ratios at the sub-nanomole level. *Journal of Physics E* 21:865–875.

Zadnik M. G., Wacker J. F., and Lewis R. S. 1985. Laboratory simulation of meteoritic noble gases; II, Sorption of xenon on carbon; etching and heating experiments. *Geochimica et Cosmochimica Acta* 49:1049–1059.

Zhang Y. and Sears D. W. G. 1996. The thermometry of enstatite chondrites: A brief review and update. *Meteoritics & Planetary Science* 31:647–655.

Zolensky M. E. and McSween H. Y. Jr. 1988. Aqueaus alteration. In *Meteorites and the early solar system*, edited by Kerridge J. F. and Mattews M. S. Tucson, Arizona: The University of Arizona Press. pp. 114–143.